STRUCTURAL CHEMISTRY

ISSN 2053-2296

High-pressure synthesis of bilayer nickelate $Sr_3Ni_2O_5Cl_2$ with a tetragonal crystal structure

Kazuki Yamane,[a,b]* Yoshitaka Matsushita,[c] Shintaro Adachi,[d] Takanobu Hiroto,[c] Ryo Matsumoto,[a] Kensei Terashima,[a] Hiroya Sakurai[a] and Yoshihiko Takano[a,b]

[a]International Center for Materials Nanoarchitectonics (MANA), National Institute for Materials Science, 1-2-1 Sengen, Tsukuba, Ibaraki 305-0047, Japan, [b]Graduate School of Pure and Applied Sciences, University of Tsukuba, 1-1-1 Tennodai, Tsukuba, Ibaraki 305-8577, Japan, [c]Research Network and Facility Services Division (RNFS), National Institute for Materials Science, 1-2-1 Sengen, Tsukuba, Ibaraki 305-0047, Japan, and [d]Nagamori Institute of Actuators, Kyoto University of Advanced Science, 18 Gotanda, Yamanouchi, Ukyo 615-8577, Japan. *Correspondence e-mail: yamane.kazuki@nims.go.jp

Received 13 December 2024
Accepted 13 March 2025

Edited by R. Diniz, Universidade Federal de Minas Gerais, Brazil

Keywords: crystal structure; superconductor; perovskite; complex anion; X-ray diffraction; Ruddlesden-Popper; oxychloride; nickel; strontium.

CCDC reference: 2431174

Supporting information: this article has supporting information at journals.iucr.org/c

Motivated by a theoretical prediction of its potential superconductivity under ambient pressure, a novel oxychloride, $Sr_3Ni_2O_5Cl_2$, was synthesized for the first time. This synthesis utilized a high pressure of 10 GPa at 1673 K. Small single crystals were used to determine the crystal structure and measure the temperature dependence of electrical resistance. The crystal is isostructural with the recently discovered superconductor $La_3Ni_2O_7$, in line with theoretical expectation.

1. Introduction

Recently, $La_3Ni_2O_7$ has been reported to exhibit superconductivity under pressures exceeding 15 GPa (Sun *et al.*, 2023). Remarkably, the superconducting transition temperature reaches as high as 80 K, comparable to that of high-T_c cuprates. The compound adopts a Ruddlesden–Popper phase structure and the superconductivity occurs in the double layers of NiO_2 square lattices like the superconductivity in CuO_2 square lattices in the cuprates. These intriguing characteristics have motivated the search for other Ni oxide superconductors (Sakakibara *et al.*, 2024*b*; Nagata *et al.*, 2024; Ueki *et al.*, 2024), with the hope that one might exhibit superconductivity at ambient pressure. This would achieve a significant breakthrough in the field.

The superconductivity of $La_3Ni_2O_7$ had been theoretically predicted even before its experimental discovery, as the intercoupling between two square lattices in the double layer is thought to be advantageous for superconductivity (Nakata *et al.*, 2017; Sakakibara *et al.*, 2024*a*; Kaneko *et al.*, 2024). Thus, the key to the occurrence of superconductivity is widely believed to lie in the Ni—O_{ap}—Ni bridging angle (Sun *et al.*, 2023), where O_{ap} represents the oxygen ion between two Ni ions along the *c* axis. In fact, the superconductivity appears above the pressure at which the orthorhombic *Amam* structure transforms into the tetragonal *I*4/*mmm* structure (Wang *et al.*, 2024*a*, 2024*b*). This transformation causes the bridging angle to change from 168 to 180°, presumably enhancing the intercoupling between the two square lattices.

Based on the same theoretical approach used to predict the superconductivity of $La_3Ni_2O_7$, the previously unreported compound $Sr_3Ni_2O_5Cl_2$ has recently been proposed as a promising candidate for a superconductor under ambient pressure (Ochi *et al.*, 2025). It is expected to exhibit tetragonal

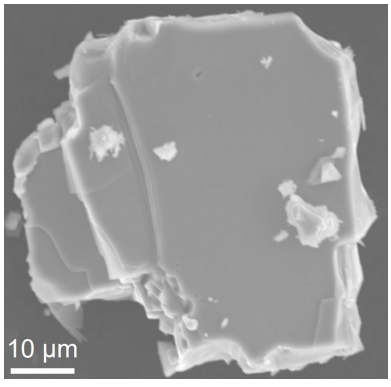

*I*4/*mmm* symmetry even under ambient pressure, if it exists. Therefore, we decided to synthesize this new Ni oxychloride and successfully obtained a single crystal. In this article, we present the method of synthesis, crystal structure and electrical resistance measurements for $Sr_3Ni_2O_5Cl_2$.

2. Experimental

2.1. Methods

Single crystals were examined using a scanning electron microscope (SEM, JSM-6010LA, JEOL) equipped with energy-dispersive X-ray spectroscopy (EDX) for elemental analysis. The compositional error in the EDX measurements was determined by measuring the same location of the crystal multiple times and calculating the standard deviation from the statistical distribution. Single-crystal X-ray diffraction (SCXRD) data were collected at 300 K using a Rigaku Synergy Custom DW single-crystal diffractometer with VariMax confocal optics for Mo *Kα* radiation (λ = 0.71073 Å) and a HyPix2000 detector. A crystal with dimensions of approximately 30 µm × 27 µm × 19 µm was isolated under paraffin oil, then immediately mounted in a dry N_2 gas stream to prevent degradation, as the compound is highly air-sensitive. Electrical resistance measurements were performed under various pressures using a diamond anvil cell (DAC) equipped with boron-doped diamond electrodes directly fabricated onto the diamond surface (Matsumoto *et al.*, 2016; Sakakibara *et al.*, 2024*b*). Resistance data were obtained with a Physical Property Measurement System (PPMS, Quantum Design).

2.2. Synthesis and crystallization

Single crystals of $Sr_3Ni_2O_5Cl_2$ were synthesized *via* high-pressure techniques using a stoichiometric mixture (1:1:1:2 molar ratio) of SrO_2, SrO, $SrCl_2$ and NiO in a Kawai-type multi-anvil press (Kawai *et al.*, 1970). SrO_2 was prepared by precipitation from a reaction between $Sr(NO_3)_2$ and H_2O_2. Specifically, $Sr(NO_3)_2$ was dissolved in deionized water that had been pre-degassed by bubbling Ar gas through it to remove dissolved CO_2. A 30% aqueous H_2O_2 solution was then added, followed by aqueous NH_3 to induce precipitation. The precipitate was filtered off and dried at 423 K. All steps were carried out in a glove bag filled with argon gas to minimize CO_2 exposure. SrO was obtained by thermal decomposition of $SrCO_3$ at 1473 K under flowing argon gas, while $SrCl_2$ was prepared by dehydrating $SrCl_2{\cdot}6H_2O$ at 573 K under vacuum. The stoichiometric mixture was sealed in a Pt capsule inside an argon-filled glove box, heated to 1673 K at 10 GPa for 2 h in the press and then the temperature was reduced to room temperature by lowering it in 100 K increments, with a 20 min hold at each step, before releasing the pressure. The final product included single crystals with typical dimensions of 50 µm × 50 µm × 30 µm.

Table 1
Experimental details.

Crystal data	
Chemical formula	$Sr_3Ni_2O_5Cl_2$
M_r	531.18
Crystal system, space group	Tetragonal, *I*4/*mmm*
Temperature (K)	301
a, *c* (Å)	3.8399 (1), 24.2936 (12)
V (Å^3)	358.21 (3)
Z	2
Radiation type	Mo *Kα*
μ (mm^{-1})	28.06
Crystal size (mm)	0.03 × 0.03 × 0.02
Data collection	
Diffractometer	Rigaku Synergy Custom DW diffractometer with a HyPix2000 detector
Absorption correction	Gaussian (*CrysAlis PRO*; Rigaku OD, 2024)
T_{min}, T_{max}	0.346, 0.380
No. of measured, independent and observed [$I > 2\sigma(I)$] reflections	8872, 500, 448
R_{int}	0.065
(sin $\theta/\lambda)_{max}$ (Å^{-1})	0.992
Refinement	
$R[F^2 > 2\sigma(F^2)]$, $wR(F^2)$, *S*	0.029, 0.076, 1.12
No. of reflections	500
No. of parameters	18
$\Delta\rho_{max}$, $\Delta\rho_{min}$ (e Å^{-3})	3.44, −1.03

Computer programs: *CrysAlis PRO* (Rigaku OD, 2024), *SHELXT2018* (Sheldrick, 2015*a*), *SHELXL2018* (Sheldrick, 2015*b*) and *OLEX2* (Dolomanov *et al.*, 2009).

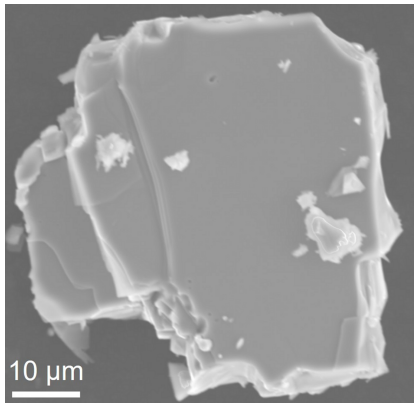

Figure 1
SEM image of a single crystal of $Sr_3Ni_2O_5Cl_2$.

3. Results and discussion

Fig. 1 shows the SEM image of a representative crystal. The plate-like morphology is consistent with the layered structure typical of the Ruddlesden–Popper phase, indicating that the crystal readily cleaves along these planes. Notably, the depicted crystal was cleaved using Scotch tape, highlighting the inherent cleavage planes of the material. EDX analysis determined the composition to be $Sr_{3.05(2)}Ni_{2.13(4)}O_xCl_{1.81(1)}$, in close agreement with the nominal stoichiometry of the starting materials.

The parameters obtained from the SCXRD structure refinements are summarized in Tables 1 and 2. No significant deviations from full occupancy were observed for any of the atoms. Consequently, the crystal structure was determined to

Table 2
Wyckoff positions (WP), occupancy (Occ), fractional atomic coordinates and isotropic and anisotropic atomic displacement parameters (Å^2) of $Sr_3Ni_2O_5Cl_2$.

Atom	WP	Occ	*x*	*y*	*z*	U_{iso}	U_{11}	U_{22}	U_{33}
Sr1	2*a*	1	0	0	0.5	0.01719 (12)	0.01381 (13)	= U_{11}	0.0239 (3)
Sr2	4*e*	1	0	0	0.34453 (2)	0.01499 (10)	0.01223 (10)	= U_{11}	0.02051 (19)
Ni	4*e*	1	0	0	0.07705 (2)	0.01226 (11)	0.01015 (13)	= U_{11}	0.01650 (2)
O_{ap}	2*a*	1	0	0	0	0.0193 (8)	0.02260 (12)	= U_{11}	0.01280 (17)
O_{eq}	8*g*	1	0	0.5	0.08818 (10)	0.0171 (4)	0.0156 (8)	0.0101 (7)	0.0256 (10)
Cl	4*e*	1	0	0	0.24750 (5)	0.0208 (2)	0.0181 (3)	= U_{11}	0.0263 (5)

be isostructural with $La_3Ni_2O_7$ and $Sr_3M_2O_5Cl_2$ (*M* = Sc, Fe and Co) (Wang *et al.*, 2024*a*, 2024*b*; Su *et al.*, 2018; Leib *et al.*, 1984; McGlothlin *et al.*, 2000). Specifically, the compound crystallizes in the Ruddlesden–Popper phase structure, adopting the tetragonal *I*4/*mmm* symmetry, with lattice parameters *a* = 3.83990 (10) and *c* = 24.2936 (12) Å, as shown in Fig. 2(*a*).

In the structure, there are two oxygen sites, 2*a* and 8*g*, referred to as O_{ap} and O_{eq}, respectively, in this article (Table 2). O_{ap} bridges two Ni atoms along the *c* axis, while O_{eq} is located between two Ni atoms in the *ab* plane. The bond lengths for Ni—O_{ap}, Ni—O_{eq} and Ni—Cl are 1.8719 (5), 1.9389 (4) and 3.1023 (14) Å, respectively. Based on these bond lengths, we have estimated the valence state of atoms

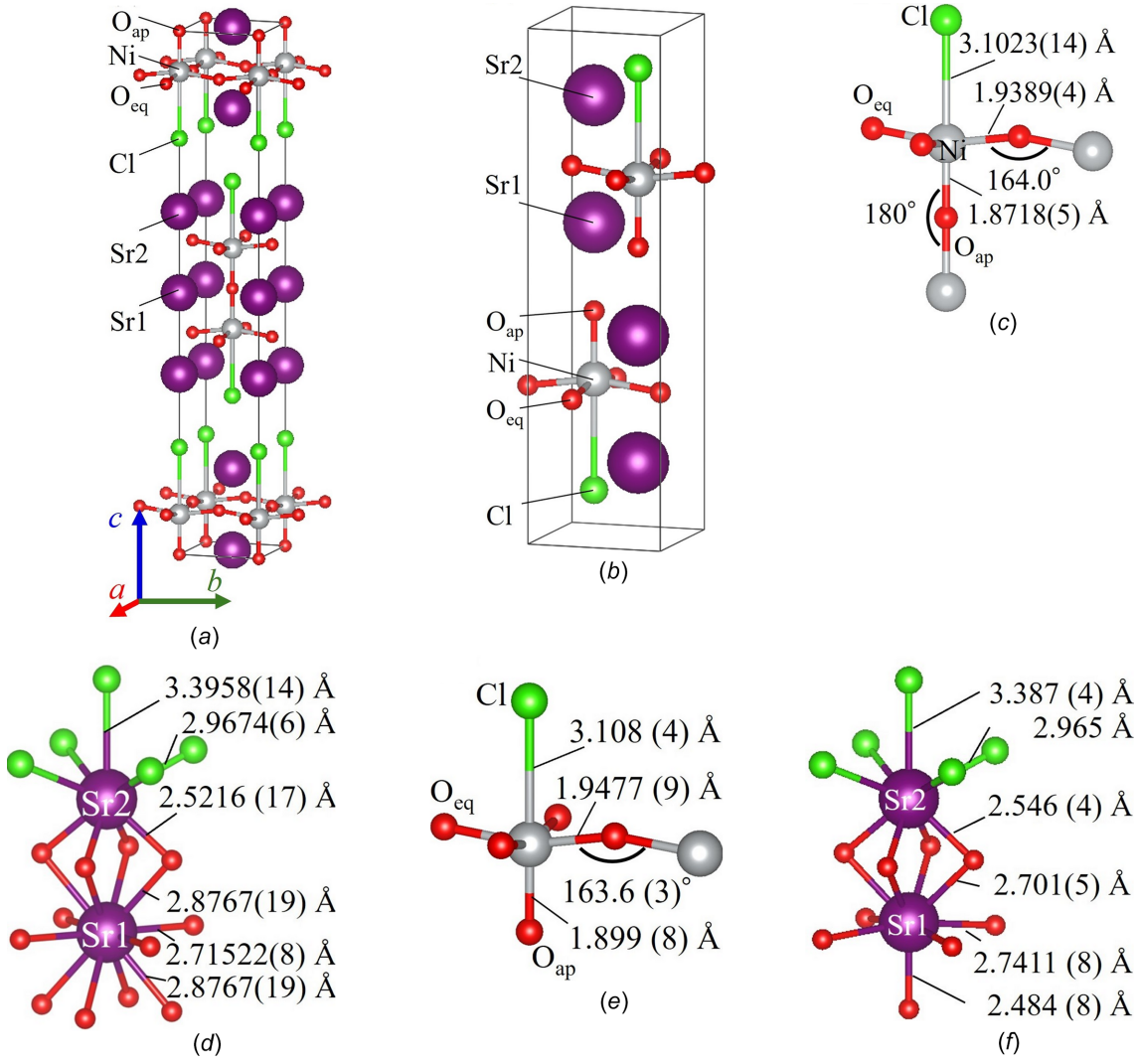

Figure 2
The crystal structures of (*a*) $Sr_3Ni_2O_5Cl_2$ and (*b*) Sr_2NiO_3Cl (Tsujimoto *et al.*, 2013), and local coordination environments around (*c*) an Ni site and (*d*) Sr sites in the former compound and (*e*)/(*f*) those in the latter compound. The boxes in panels (*a*) and (*b*) represent unit cells. These figures were created with *VESTA* (Momma & Izumi, 2011).

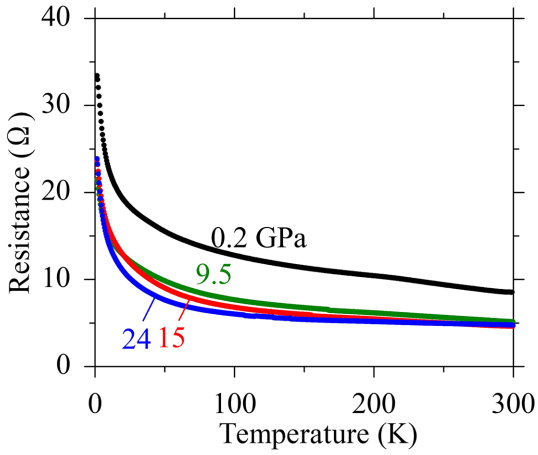

Figure 3
Temperature dependence of the electrical resistance of $Sr_3Ni_2O_5Cl_2$ under various pressures.

using the bond valence sum (BVS) method (Brown *et al.*, 1985; Brese *et al.*, 1991). The BVS parameters of $Ni^{2+}-Cl^{-}$ of 2.02 was used (Brese *et al.*, 1991), following a previous literature procedure for the related compound Sr_2NiO_3Cl (Tsujimoto *et al.*, 2013).

The Ni valence was estimated to be +3.17. Similarly, the valences of Sr1 and Sr2 were estimated from the coordination environments, shown in Fig. 2(*d*), to be +1.83 and +2.57, respectively. These values are in reasonable agreement with the formal valence expected from the composition, considering that the structure is stabilized only under high-pressure conditions (Ochi *et al.*, 2025). Another high-pressure phase of Ni oxide Sr_2NiO_3Cl (Tsujimoto *et al.*, 2013) also exhibits a larger Sr valence (+2.51) at the Sr2 site, which is surrounded by both O and Cl ions, as shown in Fig. 2(*f*). The asymmetry in coordination may account for the higher BVS valences. In contrast, the Ni ions are displaced toward the O_{ap} ions from the centre of the O_{eq} coordination plane, reducing the $Ni-O_{eq}-Ni$ bridging angle from 180 to 163.98 (15)° in $Sr_3Ni_2O_5Cl_2$. This value closely matches the theoretical prediction of 162°, further reinforcing the validity of the theoretical calculation.

Interestingly, the $Ni-O_{ap}$ bond length is significantly shorter than the $Ni-O_{eq}$ bond length. Although this trend is also observed in Sr_2NiO_3Cl, as shown in Fig. 2(*e*), it is more pronounced in $Sr_3Ni_2O_5Cl_2$. In fact, the ratio of $Ni-O_{ap}$ to $Ni-O_{eq}$ is 0.965 in $Sr_3Ni_2O_5Cl_2$, whereas the ratio for Sr_2NiO_3Cl is 0.975, suggesting stronger covalency between $Ni-O_{ap}$ in $Sr_3Ni_2O_5Cl_2$ than in Sr_2NiO_3Cl. The larger displacement of the transition-metal cations toward O_{ap} in the double-layered structure, compared to the single-layered structure, may be a common characteristic feature of strontium transition-metal oxychlorides (Hector *et al.*, 2001; Leib *et al.*, 1984; Loureiro *et al.*, 2000). Thus, the highly enhanced vertical interlayer hopping in $Sr_3Ni_2O_5Cl_2$ predicted by theory is presumably attributed to this feature of the strontium transition-metal oxychlorides, being related to the high covalence between the Ni and O_{ap} atoms.

The temperature dependences of electrical resistance under various pressures are shown in Fig. 3. Although the resistance increases with decreasing temperature at 0.2 GPa, which is almost ambient pressure, the compound remains relatively conductive, consistent with the metallic nature predicted by theory. However, no superconductivity is observed down to 2 K. The increase in resistance with decreasing temperature is gradually supressed by applying pressure up to 24 GPa, However, superconductivity does not emerge. The origin of the absence of superconductivity is under investigation.

Acknowledgements

We thank Professors Masayuki Ochi (Osaka University), Hirofumi Sakakibara (Tottori University), Hidetomo Usui (Shimane Univsity) and Kazuhiko Kuroki (Osaka University) for fruitful discussions. This work is supported by the World Premier International Research Center Initiative (WPI), MEXT, Japan, and JSPS KAKENHI.

Conflict of interest

The authors declare no competing interests.

Data availability

The authors confirm that the data supporting the findings of this study are available within the article and its supplementary materials.

Funding information

Funding for this research was provided by: World Premier International Research Center Initiative (grant No. JP20H05644); JSPS KAKENHI (grant No. JP24K01333).

References

Brese, N. E. & O'Keeffe, M. (1991). *Acta Cryst.* B**47**, 192–197.
Brown, I. D. & Altermatt, D. (1985). *Acta Cryst.* B**41**, 244–247.
Dolomanov, O. V., Bourhis, L. J., Gildea, R. J., Howard, J. A. K. & Puschmann, H. (2009). *J. Appl. Cryst.* **42**, 339–341.
Hector, A. L., Hutchings, J. A., Needs, R. L., Thomas, M. F. & Weller, M. T. (2001). *J. Mater. Chem.* **11**, 527–532.
Kaneko, T., Sakakibara, H., Ochi, M. & Kuroki, K. (2024). *Phys. Rev. B*, **109**, 045154.
Kawai, N. & Endo, S. (1970). *Rev. Sci. Instrum.* **41**, 1178–1181.
Leib, W. & Müller–Buschbaum, Hk. (1984). *Z. Anorg. Allg. Chem.* **518**, 115–119.
Loureiro, S. M., Felser, C., Huang, Q. & Cava, R. J. (2000). *Chem. Mater.* **12**, 3181–3185.
Matsumoto, R., Sasama, Y., Fujioka, M., Irifune, T., Tanaka, M., Yamaguchi, T., Takeya, H. & Takano, Y. (2016). *Rev. Sci. Instrum.* **87**, 076103.
McGlothlin, N., Ho, D. & Cava, R. J. (2000). *Mater. Res. Bull.* **35**, 1035–1043.
Momma, K. & Izumi, F. (2011). *J. Appl. Cryst.* **44**, 1272–1276.
Nagata, H., Sakurai, H., Ueki, Y., Yamane, K., Matsumoto, R., Terashima, K., Hirose, K., Ohta, H., Kato, M. & Takano, Y. (2024). *J. Phys. Soc. Jpn*, **93**, 095003.

Nakata, M., Ogura, D., Usui, H. & Kuroki, K. (2017). *Phys. Rev. B*, **95**, 214509.

Ochi, M., Sakakibara, H., Usui, H. & Kuroki, K. (2025). *Phys. Rev. B*, **111**, 064511.

Rigaku OD (2024). *CrysAlis PRO*. Rigaku Oxford Diffraction, Tokyo, Japan.

Sakakibara, H., Kitamine, N., Ochi, M. & Kuroki, K. (2024*a*). *Phys. Rev. Lett.* **132**, 106002.

Sakakibara, H., Ochi, M., Nagata, H., Ueki, Y., Sakurai, H., Matsumoto, R., Terashima, K., Hirose, K., Ohta, H., Kato, M., Takano, Y. & Kuroki, K. (2024*b*). *Phys. Rev. B*, **109**, 144511.

Sheldrick, G. M. (2015*a*). *Acta Cryst.* A**71**, 3–8.

Sheldrick, G. M. (2015*b*). *Acta Cryst.* C**71**, 3–8.

Su, Y., Tsujimoto, Y., Fujii, K., Tatsuta, M., Oka, K., Yashima, M., Ogino, H. & Yamaura, K. (2018). *Inorg. Chem.* **57**, 5615–5623.

Sun, H., Huo, M., Hu, X., Li, J., Liu, Z., Han, Y., Tang, L., Mao, Z., Yang, P., Wang, B., Cheng, J., Yao, D. X., Zhang, G. M. & Wang, M. (2023). *Nature*, **621**, 493–498.

Tsujimoto, Y., Yamaura, K. & Uchikoshi, T. (2013). *Inorg. Chem.* **52**, 10211–10216.

Ueki, Y., Sakurai, H., Nagata, H., Yamane, K., Matsumoto, R., Terashima, K., Hirose, K., Ohta, H., Kato, M. & Takano, Y. (2024). arXiv preprint arXiv:2408.04970.

Wang, L., Li, Y., Xie, S. Y., Liu, F., Sun, H., Huang, C., Gao, Y., Nakagawa, T., Fu, B., Dong, B., Cao, Z., Yu, R., Kawaguchi, S. I., Kadobayashi, H., Wang, M., Jin, C., Mao, H. K. & Liu, H. (2024*a*). *J. Am. Chem. Soc.* **146**, 7506–7514.

Wang, N., Wang, G., Shen, X., Hou, J., Luo, J., Ma, X., Yang, H., Shi, L., Dou, J., Feng, J., Yang, J., Shi, Y., Ren, Z., Ma, H., Yang, P., Liu, Y., Liu, Y., Zhang, H., Dong, X., Wang, Y., Jiang, K., Hu, J., Nagasaki, S., Kitagawa, K., Calder, S., Yan, J., Sun, J., Wang, B., Zhou, R., Uwatoko, Y. & Cheng, J. (2024*b*). *Nature*, **634**, 579–584.

supporting information

Acta Cryst. (2025). C**81**, 259-263 [https://doi.org/10.1107/S2053229625002281]

High-pressure synthesis of bilayer nickelate $Sr_3Ni_2O_5Cl_2$ with a tetragonal crystal structure

Kazuki Yamane, Yoshitaka Matsushita, Shintaro Adachi, Takanobu Hiroto, Ryo Matsumoto, Kensei Terashima, Hiroya Sakurai and Yoshihiko Takano

Computing details

Tristrontium dinickel pentaoxide dichloride

Crystal data

$Sr_3Ni_2O_5Cl_2$
M_r = 531.18
Tetragonal, *I*4/*mmm*
a = 3.8399 (1) Å
c = 24.2936 (12) Å
V = 358.21 (3) Å^3
Z = 2
F(000) = 488
D_x = 4.925 Mg m^{-3}
Mo *Kα* radiation, *λ* = 0.71073 Å
Cell parameters from 4484 reflections
θ = 3.3–44.7°
μ = 28.06 mm^{-1}
T = 301 K
Block, metallic black
0.03 × 0.03 × 0.02 mm

Data collection

Rigaku Synergy Custom DW diffractometer with a HyPix2000 detector
Radiation source: Rotating-anode X-ray tube, Rigaku (Mo) X-ray Source
Mirror monochromator
Detector resolution: 10.0000 pixels mm^{-1}
ω scans
Absorption correction: gaussian (CrysAlis PRO; Rigaku OD, 2024)
T_{min} = 0.346, T_{max} = 0.380
8872 measured reflections
500 independent reflections
448 reflections with $I > 2\sigma(I)$
R_{int} = 0.065
θ_{max} = 44.9°, θ_{min} = 3.4°
h = −7→7
k = −7→7
l = −48→48

Refinement

Refinement on F^2
Least-squares matrix: full
$R[F^2 > 2\sigma(F^2)]$ = 0.029
$wR(F^2)$ = 0.076
S = 1.12
500 reflections
18 parameters
0 restraints
Primary atom site location: dual
$w = 1/[\sigma^2(F_o^2) + (0.0395P)^2 + 0.6699P]$ where $P = (F_o^2 + 2F_c^2)/3$
$(\Delta/\sigma)_{max}$ = 0.001
$\Delta\rho_{max}$ = 3.44 e Å^{-3}
$\Delta\rho_{min}$ = −1.03 e Å^{-3}

Special details

Geometry. All esds (except the esd in the dihedral angle between two l.s. planes) are estimated using the full covariance matrix. The cell esds are taken into account individually in the estimation of esds in distances, angles and torsion angles; correlations between esds in cell parameters are only used when they are defined by crystal symmetry. An approximate (isotropic) treatment of cell esds is used for estimating esds involving l.s. planes.

Fractional atomic coordinates and isotropic or equivalent isotropic displacement parameters (Å²)

	x	*y*	*z*	U_{iso}*/U_{eq}
Ni	−0.500000	−0.500000	0.42295 (2)	0.01226 (11)
O1	−0.500000	−0.500000	0.500000	0.0193 (8)
O2	−0.500000	−1.000000	0.41182 (10)	0.0171 (4)
Cl	−0.500000	−0.500000	0.29525 (5)	0.0208 (2)
Sr1	0.000000	0.000000	0.500000	0.01719 (12)
Sr2	−1.000000	−1.000000	0.34453 (2)	0.01499 (10)

Atomic displacement parameters (Å²)

	U^{11}	U^{22}	U^{33}	U^{12}	U^{13}	U^{23}
Ni	0.01015 (13)	0.01015 (13)	0.0165 (2)	0.000	0.000	0.000
O1	0.0226 (12)	0.0226 (12)	0.0128 (17)	0.000	0.000	0.000
O2	0.0156 (8)	0.0101 (7)	0.0256 (10)	0.000	0.000	0.000
Cl	0.0181 (3)	0.0181 (3)	0.0263 (5)	0.000	0.000	0.000
Sr1	0.01381 (13)	0.01381 (13)	0.0239 (3)	0.000	0.000	0.000
Sr2	0.01223 (10)	0.01223 (10)	0.02051 (19)	0.000	0.000	0.000

Geometric parameters (Å, º)

Ni—O1	1.8719 (5)	O1—Sr1^{vi}	2.7152 (1)
Ni—O2	1.9389 (3)	O1—Sr1^{v}	2.7152 (1)
Ni—O2^{i}	1.9389 (4)	O1—Sr1^{iv}	2.7152 (1)
Ni—O2^{ii}	1.9389 (4)	O2—Sr1^{vi}	2.8766 (18)
Ni—O2^{iii}	1.9389 (4)	O2—Sr1^{iv}	2.8766 (18)
Ni—Sr1	3.2980 (3)	O2—Sr2	2.5217 (16)
Ni—Sr1^{iv}	3.2980 (3)	O2—Sr2^{viii}	2.5218 (16)
Ni—Sr1^{v}	3.2980 (3)	Cl—Sr2^{vii}	2.9674 (6)
Ni—Sr1^{vi}	3.2980 (3)	Cl—Sr2^{viii}	2.9674 (6)
Ni—Sr2	3.3169 (4)	Cl—Sr2	2.9674 (6)
Ni—Sr2^{vii}	3.3169 (4)	Cl—Sr2^{ix}	3.3956 (13)
Ni—Sr2^{viii}	3.3169 (4)	Cl—Sr2^{iii}	2.9674 (6)
O1—Sr1	2.7152 (1)		
O1—Ni—O2	98.01 (7)	O1—Sr1—O2^{xiv}	118.16 (2)
O1—Ni—O2^{i}	98.01 (7)	O1^{vii}—Sr1—O2^{iii}	118.16 (2)
O1—Ni—O2^{ii}	98.01 (7)	O1—Sr1—O2^{ii}	61.84 (2)
O1—Ni—O2^{iii}	98.01 (7)	O1^{iii}—Sr1—O2^{iii}	61.84 (2)
O1—Ni—Sr1	55.417 (8)	O1—Sr1—O2^{iii}	61.84 (2)
O1—Ni—Sr1^{vi}	55.417 (8)	O1^{iii}—Sr1—O2^{ii}	118.16 (2)
O1—Ni—Sr1^{iv}	55.417 (7)	O1—Sr1—O2^{xiii}	61.84 (2)
O1—Ni—Sr1^{v}	55.417 (8)	O1^{viii}—Sr1—O2^{iii}	118.16 (2)
O1—Ni—Sr2	125.055 (9)	O1^{viii}—Sr1—O2^{xii}	118.16 (2)
O1—Ni—Sr2^{vii}	125.056 (9)	O1^{vii}—Sr1—O2^{x}	118.16 (2)
O1—Ni—Sr2^{viii}	125.056 (9)	O1^{viii}—Sr1—O2^{xiv}	61.84 (2)
O2^{i}—Ni—O2^{ii}	163.98 (15)	O1^{iii}—Sr1—O2^{x}	61.84 (2)

O2—Ni—O2^{i}	88.89 (2)	O1^{viii}—Sr1—O2^{x}	118.16 (2)
O2—Ni—O2^{ii}	88.89 (2)	O1^{vii}—Sr1—O2^{vii}	61.84 (2)
O2^{i}—Ni—O2^{iii}	88.89 (2)	O1—Sr1—O2^{x}	61.84 (2)
O2—Ni—O2^{iii}	163.98 (15)	O1^{iii}—Sr1—O2^{vii}	118.16 (2)
O2^{ii}—Ni—O2^{iii}	88.89 (2)	O1^{viii}—Sr1—O2^{vii}	61.84 (2)
O2^{i}—Ni—Sr1^{v}	60.17 (5)	O1^{vii}—Sr1—O2^{xiii}	118.16 (2)
O2—Ni—Sr1	130.96 (5)	O1—Sr1—O2^{xi}	118.16 (2)
O2^{ii}—Ni—Sr1^{v}	130.96 (5)	O1^{iii}—Sr1—O2^{xiii}	118.16 (2)
O2^{i}—Ni—Sr1	130.96 (5)	O1—Sr1—O2^{vii}	118.16 (2)
O2—Ni—Sr1^{vi}	60.17 (5)	O1^{vii}—Sr1—O2^{xii}	61.84 (2)
O2^{ii}—Ni—Sr1	60.17 (5)	O1^{iii}—Sr1—O2^{xiv}	118.16 (2)
O2^{ii}—Ni—Sr1^{vi}	60.17 (5)	O1^{iii}—Sr1—O2^{xii}	61.84 (2)
O2^{i}—Ni—Sr1^{vi}	130.96 (5)	O1^{vii}—Sr1—O2^{xiv}	61.84 (2)
O2^{iii}—Ni—Sr1^{v}	60.17 (5)	O2^{xiv}—Sr1—O2^{iii}	180.0
O2^{iii}—Ni—Sr1^{vi}	130.96 (5)	O2^{xi}—Sr1—O2^{iii}	123.68 (4)
O2^{i}—Ni—Sr1^{iv}	60.17 (5)	O2^{xiv}—Sr1—O2^{xiii}	56.32 (4)
O2^{ii}—Ni—Sr1^{iv}	130.96 (5)	O2^{ii}—Sr1—O2^{xiv}	123.68 (4)
O2^{iii}—Ni—Sr1^{iv}	130.96 (5)	O2^{iii}—Sr1—O2^{vii}	83.74 (7)
O2—Ni—Sr1^{iv}	60.17 (5)	O2^{ii}—Sr1—O2^{iii}	56.32 (4)
O2—Ni—Sr1^{v}	130.96 (5)	O2^{xiv}—Sr1—O2^{xii}	123.68 (4)
O2^{iii}—Ni—Sr1	60.17 (5)	O2^{iii}—Sr1—O2^{xiii}	123.68 (4)
O2^{iii}—Ni—Sr2	119.55 (6)	O2^{iii}—Sr1—O2^{xii}	56.32 (4)
O2—Ni—Sr2	49.21 (5)	O2^{xi}—Sr1—O2^{x}	56.32 (4)
O2^{ii}—Ni—Sr2	119.55 (6)	O2^{xiii}—Sr1—O2^{xii}	180.0
O2—Ni—Sr2^{vii}	119.55 (6)	O2^{xiv}—Sr1—O2^{x}	83.74 (7)
O2^{i}—Ni—Sr2^{viii}	119.55 (6)	O2^{iii}—Sr1—O2^{x}	96.26 (7)
O2^{i}—Ni—Sr2	49.21 (5)	O2^{xi}—Sr1—O2^{xiv}	56.32 (4)
O2—Ni—Sr2^{viii}	49.21 (5)	O2^{xi}—Sr1—O2^{xii}	96.26 (7)
O2^{iii}—Ni—Sr2^{viii}	119.55 (6)	O2^{ii}—Sr1—O2^{xiii}	96.26 (7)
O2^{ii}—Ni—Sr2^{viii}	49.21 (5)	O2^{xi}—Sr1—O2^{vii}	123.68 (4)
O2^{i}—Ni—Sr2^{vii}	119.55 (6)	O2^{xi}—Sr1—O2^{xiii}	83.74 (7)
O2^{iii}—Ni—Sr2^{vii}	49.21 (5)	O2^{ii}—Sr1—O2^{vii}	56.32 (4)
O2^{ii}—Ni—Sr2^{vii}	49.21 (5)	O2^{xiv}—Sr1—O2^{vii}	96.26 (7)
Sr1^{v}—Ni—Sr1^{iv}	71.206 (7)	O2^{xiii}—Sr1—O2^{vii}	123.68 (4)
Sr1^{vi}—Ni—Sr1^{iv}	71.206 (7)	O2^{ii}—Sr1—O2^{x}	123.68 (4)
Sr1^{v}—Ni—Sr1^{vi}	110.833 (15)	O2^{ii}—Sr1—O2^{xii}	83.74 (7)
Sr1—Ni—Sr1^{v}	71.206 (7)	O2^{xii}—Sr1—O2^{vii}	56.32 (4)
Sr1—Ni—Sr1^{vi}	71.206 (7)	O2^{xiii}—Sr1—O2^{x}	56.32 (4)
Sr1—Ni—Sr1^{iv}	110.833 (15)	O2^{x}—Sr1—O2^{vii}	180.0
Sr1^{v}—Ni—Sr2^{vii}	109.027 (3)	O2^{xii}—Sr1—O2^{x}	123.68 (4)
Sr1^{vi}—Ni—Sr2^{viii}	69.639 (7)	O2^{xi}—Sr1—O2^{ii}	180.0
Sr1—Ni—Sr2	179.528 (15)	Ni^{v}—Sr2—Ni^{iv}	70.737 (9)
Sr1^{v}—Ni—Sr2	109.027 (3)	Ni^{vi}—Sr2—Ni^{iv}	70.737 (9)
Sr1^{iv}—Ni—Sr2	69.638 (7)	Ni—Sr2—Ni^{v}	70.737 (9)
Sr1^{iv}—Ni—Sr2^{vii}	179.528 (15)	Ni—Sr2—Ni^{vi}	70.737 (9)
Sr1—Ni—Sr2^{vii}	69.639 (7)	Ni^{v}—Sr2—Ni^{vi}	109.889 (18)
Sr1—Ni—Sr2^{viii}	109.027 (3)	Ni—Sr2—Ni^{iv}	109.889 (18)
Sr1^{v}—Ni—Sr2^{viii}	179.528 (15)	O2—Sr2—Ni^{iv}	93.92 (4)

Sr1^{iv}—Ni—Sr2^{viii}	109.027 (3)	O2—Sr2—Ni^{v}	93.92 (4)
Sr1^{vi}—Ni—Sr2^{vii}	109.027 (3)	O2^{xv}—Sr2—Ni^{vi}	35.602 (6)
Sr1^{vi}—Ni—Sr2	109.027 (3)	O2^{i}—Sr2—Ni^{vi}	93.92 (4)
Sr2—Ni—Sr2^{viii}	70.737 (9)	O2^{xv}—Sr2—Ni^{v}	93.92 (4)
Sr2—Ni—Sr2^{vii}	109.889 (18)	O2^{i}—Sr2—Ni^{iv}	93.92 (4)
Sr2^{vii}—Ni—Sr2^{viii}	70.737 (9)	O2^{v}—Sr2—Ni^{iv}	35.602 (6)
Ni^{x}—O1—Ni	180.0	O2—Sr2—Ni	35.602 (6)
Ni—O1—Sr1^{iv}	90.0	O2^{xv}—Sr2—Ni	93.92 (4)
Ni^{x}—O1—Sr1^{v}	90.0	O2^{xv}—Sr2—Ni^{iv}	35.602 (6)
Ni^{x}—O1—Sr1^{vi}	90.0	O2^{v}—Sr2—Ni^{v}	35.602 (6)
Ni^{x}—O1—Sr1	90.0	O2^{i}—Sr2—Ni	35.602 (6)
Ni—O1—Sr1^{v}	90.0	O2^{v}—Sr2—Ni	93.92 (4)
Ni—O1—Sr1^{vi}	90.0	O2^{i}—Sr2—Ni^{v}	35.602 (6)
Ni^{x}—O1—Sr1^{iv}	90.0	O2—Sr2—Ni^{vi}	35.602 (6)
Ni—O1—Sr1	90.0	O2^{v}—Sr2—Ni^{vi}	93.92 (4)
Sr1^{v}—O1—Sr1^{vi}	180.0	O2^{v}—Sr2—O2	99.17 (9)
Sr1—O1—Sr1^{vi}	90.0	O2^{i}—Sr2—O2^{v}	65.14 (5)
Sr1^{iv}—O1—Sr1	180.0	O2^{i}—Sr2—O2^{xv}	99.17 (9)
Sr1^{iv}—O1—Sr1^{vi}	90.0	O2^{i}—Sr2—O2	65.14 (5)
Sr1—O1—Sr1^{v}	90.0	O2^{xv}—Sr2—O2	65.14 (5)
Sr1^{iv}—O1—Sr1^{v}	90.0	O2^{xv}—Sr2—O2^{v}	65.14 (5)
Ni—O2—Ni^{vi}	163.98 (15)	O2^{v}—Sr2—Cl	138.952 (17)
Ni^{vi}—O2—Sr1^{vi}	84.04 (6)	O2^{i}—Sr2—Cl^{iv}	138.952 (17)
Ni^{vi}—O2—Sr1^{iv}	84.04 (6)	O2—Sr2—Cl	76.64 (4)
Ni—O2—Sr1^{iv}	84.04 (6)	O2^{i}—Sr2—Cl	76.64 (4)
Ni—O2—Sr1^{vi}	84.04 (6)	O2^{v}—Sr2—Cl^{v}	76.64 (4)
Ni—O2—Sr2	95.18 (4)	O2^{v}—Sr2—Cl^{iv}	76.64 (4)
Ni—O2—Sr2^{viii}	95.18 (4)	O2—Sr2—Cl^{iv}	138.952 (17)
Ni^{vi}—O2—Sr2	95.18 (4)	O2^{xv}—Sr2—Cl^{iv}	76.64 (4)
Ni^{vi}—O2—Sr2^{viii}	95.18 (4)	O2—Sr2—Cl^{vi}	76.64 (4)
Sr1^{vi}—O2—Sr1^{iv}	83.74 (7)	O2^{xv}—Sr2—Cl^{vi}	76.64 (4)
Sr2—O2—Sr1^{iv}	88.546 (13)	O2^{i}—Sr2—Cl^{v}	76.64 (4)
Sr2^{viii}—O2—Sr1^{iv}	172.29 (8)	O2^{v}—Sr2—Cl^{vi}	138.952 (17)
Sr2—O2—Sr1^{vi}	172.28 (8)	O2^{i}—Sr2—Cl^{vi}	138.952 (17)
Sr2^{viii}—O2—Sr1^{vi}	88.547 (13)	O2^{xv}—Sr2—Cl^{v}	138.952 (17)
Sr2—O2—Sr2^{viii}	99.17 (9)	O2^{xv}—Sr2—Cl	138.952 (17)
Sr2^{vii}—Cl—Sr2^{iii}	80.635 (18)	O2—Sr2—Cl^{v}	138.952 (17)
Sr2^{iii}—Cl—Sr2	80.634 (18)	Cl^{iv}—Sr2—Ni	168.74 (3)
Sr2^{viii}—Cl—Sr2	80.634 (18)	Cl^{iv}—Sr2—Ni^{iv}	58.85 (2)
Sr2^{iii}—Cl—Sr2^{ix}	113.79 (2)	Cl^{vi}—Sr2—Ni^{v}	168.74 (3)
Sr2—Cl—Sr2^{ix}	113.79 (2)	Cl—Sr2—Ni^{vi}	103.398 (13)
Sr2^{vii}—Cl—Sr2^{viii}	80.635 (18)	Cl^{v}—Sr2—Ni^{iv}	103.398 (13)
Sr2^{iii}—Cl—Sr2^{viii}	132.42 (5)	Cl—Sr2—Ni^{v}	103.398 (13)
Sr2^{vii}—Cl—Sr2^{ix}	113.79 (2)	Cl^{vi}—Sr2—Ni^{iv}	103.398 (13)
Sr2^{vii}—Cl—Sr2	132.42 (5)	Cl^{iv}—Sr2—Ni^{v}	103.398 (13)
Sr2^{viii}—Cl—Sr2^{ix}	113.79 (2)	Cl^{v}—Sr2—Ni^{vi}	168.74 (3)
O1^{vii}—Sr1—O1	180.0	Cl^{v}—Sr2—Ni	103.397 (13)
O1—Sr1—O1^{iii}	90.0	Cl^{iv}—Sr2—Ni^{vi}	103.398 (13)

O1—Sr1—O1^{viii}	90.0	Cl^{vi}—Sr2—Ni^{vi}	58.85 (2)
O1^{vii}—Sr1—O1^{viii}	90.0	Cl—Sr2—Ni	58.85 (2)
O1^{iii}—Sr1—O1^{viii}	180.0	Cl—Sr2—Ni^{iv}	168.74 (3)
O1^{vii}—Sr1—O1^{iii}	90.0	Cl^{v}—Sr2—Ni^{v}	58.85 (2)
O1^{vii}—Sr1—O2^{xi}	61.84 (2)	Cl^{vi}—Sr2—Ni	103.397 (13)
O1—Sr1—O2^{xii}	118.16 (2)	Cl^{v}—Sr2—Cl^{vi}	132.42 (5)
O1^{viii}—Sr1—O2^{xi}	118.16 (2)	Cl^{iv}—Sr2—Cl^{vi}	80.634 (18)
O1^{vii}—Sr1—O2^{ii}	118.16 (2)	Cl—Sr2—Cl^{v}	80.634 (18)
O1^{iii}—Sr1—O2^{xi}	61.84 (2)	Cl—Sr2—Cl^{vi}	80.634 (18)
O1^{viii}—Sr1—O2^{ii}	61.84 (2)	Cl^{iv}—Sr2—Cl^{v}	80.634 (18)
O1^{viii}—Sr1—O2^{xiii}	61.84 (2)	Cl^{iv}—Sr2—Cl	132.42 (5)
O2—Ni—O1—Sr1^{iv}	−45.0	Sr1^{iv}—Ni—O1—Sr1^{vi}	90.0
O2—Ni—O1—Sr1^{v}	−135.0	Sr1^{vi}—Ni—O1—Sr1^{v}	180.0
O2^{iii}—Ni—O1—Sr1^{iv}	135.0	Sr1—Ni—O1—Sr1^{vi}	−90.0
O2—Ni—O1—Sr1	135.0	Sr1^{v}—Ni—O1—Sr1	−90.0
O2^{ii}—Ni—O1—Sr1^{iv}	−135.0	Sr1—Ni—O1—Sr1^{v}	90.0
O2^{iii}—Ni—O1—Sr1	−45.0	Sr1^{vi}—Ni—O1—Sr1^{iv}	−90.0
O2—Ni—O1—Sr1^{vi}	45.0	Sr1^{iv}—Ni—O1—Sr1	180.0
O2^{iii}—Ni—O1—Sr1^{vi}	−135.0	Sr1^{vi}—Ni—O1—Sr1	90.0
O2^{i}—Ni—O1—Sr1^{v}	−45.0	Sr2^{vii}—Ni—O1—Sr1^{v}	90.0
O2^{i}—Ni—O1—Sr1	−135.0	Sr2^{viii}—Ni—O1—Sr1^{iv}	−90.0
O2^{ii}—Ni—O1—Sr1^{v}	135.0	Sr2^{viii}—Ni—O1—Sr1^{v}	180.0
O2^{iii}—Ni—O1—Sr1^{v}	45.0	Sr2^{vii}—Ni—O1—Sr1	0.0
O2^{i}—Ni—O1—Sr1^{iv}	45.0	Sr2^{vii}—Ni—O1—Sr1^{vi}	−90.0
O2^{ii}—Ni—O1—Sr1	45.0	Sr2—Ni—O1—Sr1	180.0
O2^{i}—Ni—O1—Sr1^{vi}	135.0	Sr2^{vii}—Ni—O1—Sr1^{iv}	180.0
O2^{ii}—Ni—O1—Sr1^{vi}	−45.0	Sr2—Ni—O1—Sr1^{vi}	90.0
Sr1—Ni—O1—Sr1^{iv}	180.0	Sr2^{viii}—Ni—O1—Sr1^{vi}	0.0
Sr1^{iv}—Ni—O1—Sr1^{v}	−90.0	Sr2^{viii}—Ni—O1—Sr1	90.0
Sr1^{v}—Ni—O1—Sr1^{vi}	180.0	Sr2—Ni—O1—Sr1^{v}	−90.0
Sr1^{v}—Ni—O1—Sr1^{iv}	90.0	Sr2—Ni—O1—Sr1^{iv}	0.0

Symmetry codes: (i) −*y*−2, *x*, *z*; (ii) −*y*−1, *x*, *z*; (iii) *x*, *y*+1, *z*; (iv) *x*−1, *y*−1, *z*; (v) *x*−1, *y*, *z*; (vi) *x*, *y*−1, *z*; (vii) *x*+1, *y*+1, *z*; (viii) *x*+1, *y*, *z*; (ix) −*x*−3/2, −*y*−3/2, −*z*+1/2; (x) −*x*−1, −*y*−1, −*z*+1; (xi) *y*+1, −*x*, −*z*+1; (xii) −*y*−1, *x*+1, *z*; (xiii) *y*+1, −*x*−1, −*z*+1; (xiv) −*x*, −*y*−1, −*z*+1; (xv) −*y*−2, *x*−1, *z*.